Macromolecules 1991, *24,* 6306–6309

Effect of Polymer Matrix on the Oxygen Diffusion via a Cobalt Porphyrin Fixed in a Membrane

Hiroyuki Nishide, Hiroyoshi Kawakami, Takayuki Suzuki, Yasutaka Azechi, Yuji Soejima, and Eishun Tsuchida*

Department of Polymer Chemistry, Waseda University, Tokyo 169, Japan

Received March 19, 1991; Revised Manuscript Received July 8, 1991

ABSTRACT: Specific and facilitated transport of molecular oxygen through a polymer membrane containing [α-mono(*o*-methacrylamidophenyl)-α,α,α-tris(*o*-pivalamidophenyl)porphinato]cobalt (CoMPP) complex as a fixed oxygen carrier is analyzed by a modified dual-mode transport theory, and the effect of the polymer matrix on the oxygen diffusion via the fixed carrier is discussed. Oxygen diffusion coefficients for the diffusion from the polymer matrix to the fixed carrier (D_{DC}) and for the diffusion from the fixed carrier to the polymer matrix (D_{CD}) increase with physical diffusivity through the polymer matrix. In contrast, the oxygen diffusion coefficient for hopping between the fixed carriers (D_{CC}) is independent of the polymer matrix species.

Introduction

We have reported highly selective transport of oxygen through polymer membranes containing a cobalt porphyrin (CoP) and a cobalt Schiff base (CoS) as fixed oxygen carriers.[1-6] The permeability coefficient ratio of oxygen against nitrogen was >10 through membranes containing a large amount of the fixed carriers. Recently, we succeeded in synthesizing [α-mono(*o*-methacrylamidophenyl)-α,α,α-tris(*o*-pivalamidophenyl)porphinato]cobalt[7] (CoMPP (1)), a cobalt porphyrin derivatives with an improved oxygen-binding equilibrium and kinetic ability as the fixed oxygen carrier in comparison with those of [*meso*-$\alpha,\alpha,\alpha,\alpha$-tetrakis(*o*-pivalamidophenyl)porphinato]cobalt. The improved carrier enables not only a higher permselectivity[7] but also a more precise study of the selective and facilitated oxygen transport in the polymer membranes.

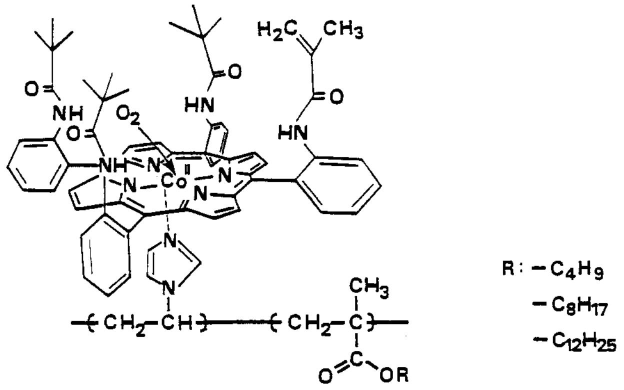

1

The facilitated transport of oxygen in membranes has been described by a dual-mode transport model: The oxygen permeability coefficient is represented as the sum of the Henry mode, described by the physical permeation, and the Langmuir mode, described by the specific binding and the diffusion of oxygen to and through the fixed carrier.[2,5] Recently, mathematical modification of this dual-mode transport model has also been proposed.[8-10] Analysis of the facilitated transport by the modified model will elaborate the oxygen diffusion profile via the fixed carrier in the membrane.

In this paper, we describe the oxygen diffusions via the fixed carrier CoMPP in polymer membranes analyzed by a modified dual-mode transport model and the effect of the polymer matrices on them. The polymers used were poly(butyl methacrylate-*co*-1-vinylimidazole), poly(octyl methacrylate-*co*-1-vinylimidazole), and poly(lauryl methacrylate-*co*-1-vinylimidazole) (BIm, OIm, and LIm, respectively). The vinylimidazole residue of the copolymers combines with the fifth coordination site of CoMPP, as shown in 1, not only to afford oxygen-binding capability to CoMPP (oxygen binds to the sixth coordination site) but also to fix CoMPP on the polymer chain (CoMPP is homogeneously dispersed in the membrane). The character of the oxygen binding and the contribution of the fixed carrier CoMPP complex to permselectivity are also described.

Experimental Section

Material. [α-Mono(*o*-methacrylamidophenyl)-α,α,α-tris(*o*-pivalamidophenyl)porphinato]cobalt was synthesized by reaction of [*meso*-$\alpha,\alpha,\alpha,\alpha$-tetrakis(*o*-aminophenyl)porphinato]cobalt with a mixture of methacryl chloride and pivaloyl chloride. The copolymers, BIm, OIm, and LIm, were prepared by the radical polymerization of 1-vinylimidazole with butyl methacrylate, octyl methacrylate, and lauryl methacrylate, respectively. The 1-vinylimidazole residue contents and the molecular weights of the copolymers were determined to be 11 mol % (7.6 wt %) and 1.8×10^5 for BIm, 16 mol % (8.3 wt %) and 2.0×10^5 for OIm, and 21 mol % (9.0 wt %) and 1.5×10^5 for LIm by elemental analysis and gel permeation chromatography (with tetrahydrofuran as the solvent and polystyrene as the standard), respectively. CoMPP was combined with the copolymers in their chloroform solution, and the chloroform solution was carefully cast on a Teflon plate under an oxygen-free atmosphere and dried in vacuo to yield a transparent and flexible membrane with thickness of ca. 60 μm.

Spectroscopic and Permeation Measurements. Oxygen binding to the CoMPP complex fixed in the solid membrane was observed by a spectral change in the visible absorption using a spectrophotometer (Shimadzu Model UV 2100). Photodissociation and recombination of bound oxygen from and to CoMPP in the membrane were monitored in situ by laser flash photolysis, as described in the previous paper,[5] with a rapid and sensitive spectrophotometer (Unisok FR-2000).

Oxygen and nitrogen permeation coefficients for various upstream gas pressures were measured with a low-vacuum permeation apparatus (Rika Seiki Inc. Model K-315-N) in the temperature range 5–55 °C.

Results and Discussion

Oxygen Binding in the CoMPP Complex Fixed in the Membrane. A membrane sample was attached to the cell wall of the spectrophotometer, and a gaseous

0024-9297/91/2224-6306$02.50/0

Table I
Oxygen-Binding Equilibrium Constant and Thermodynamic and Kinetic Parameters for the CoMPP Membranes at 25 °C

polymer	T_g[a]	$10K_{app}$[b]	10^3k_D[c]	$10^{-3}K$[d]	ΔH[e]	ΔS[f]	$10^3k'_{on}$[g]	$10^3k'_{off}$[h]	$10^{-7}k_{on}$[i]	$10^{-3}k_{off}$[j]
BIm	30	2.1	1.0	4.8	−12	−35	1.3	6.8	1.7	3.5
OIm	0	3.1	1.5	5.2	−13	−37	2.9	9.3	1.9	3.7
LIm	−23	3.8	1.7	5.0	−13	−37	3.9	10	1.8	3.6

[a] °C. [b] 1/cmHg. [c] cm^3 (STP)/(cm^3 cmHg). [d] 1/*M*. [e] kcal/mol. [f] eu. [g] 1/(cmHg s). [h] 1/s. [i] 1/(M s). [j] 1/s.

Table II
Dual-Mode Transport Parameters for the CoMPP Membranes at 45 °C

polymer	10^4k_D[a]	C_C'[b]	10^6D_{DD}[c]	10^7D_{DC}[c]	10^8D_{CD}[c]	10^9D_{CC}[c]
BIm	6.1	0.14	1.6	1.9	1.3	7.9
OIm	7.8	0.13	2.4	2.2	1.5	7.9
LIm	7.9	0.13	6.2	2.9	2.6	7.9

[a] cm^3 (STP)/(cm^3·cmHg). [b] cm^3 (STP)/cm^3. [c] cm^2/s.

mixture of oxygen and nitrogen was introduced into the cell with a stand pressure such that the total pressure in the cell was 1 atm. The visible absorption (λ_{max} = 528 nm) assigned to the deoxy CoMPP complex was reversibly changed to the absorption (λ_{max} = 548 nm) assigned to the oxy CoMPP complex (Co/O_2 = 1/1 adduct) with isosbestic points at 480, 538, and 667 nm in response to the partial pressure of oxygen. The apparent oxygen-binding equilibrium constant (K_{app} ($cmHg^{-1}$)) was determined by conducting a Langmuir-type oxygen-binding equilibrium measurement and is given in Table I. Enthalpy and entropy changes for the oxygen binding were estimated from the temperature dependence of K (5–55 °C) and are also listed in Table I. The K_{app} value is enhanced with decreasing T_g or increasing oxygen solubility in the polymer matrix. That is, K_{app} is a good indication of the oxygen solubility or the free volume of the polymer matrices.

The oxygen-binding equilibrium constant K ($L{\cdot}mol^{-1}$) can be derived from the correction of K_{app} by the physical oxygen dissolution in a polymer matrix as

$$K = [Co\text{-}O_2]/[Co][O_2] \tag{1}$$

$$K = K_{app}/k_D \tag{2}$$

where $[O_2]$ (cm^3 (STP)$\cdot cm^{-3}$ or $mol{\cdot}L^{-1}$) = $k_Dp(O_2)$ is the oxygen concentration around the complex in a membrane, k_D is the oxygen solubility coefficient (cm^3 (STP)$\cdot cm^{-3}\cdot cmHg^{-1}$) (estimated in this paper through the permeation measurement in Table II), and $p(O_2)$ is the partial pressure of oxygen (cmHg) to which a membrane is exposed. The converted K values in Table I are hardly affected by the polymer matrix species, or the oxygen-binding equilibrium of the complex itself is essentially independent of the surrounding polymer.

The oxygen binding and dissociation occurred very rapidly: For a 60-μm membrane containing 1.3 wt % CoMPP the binding equilibrium was established within a few minutes after exposure to oxygen or nitrogen. The time courses of the degree of oxygen binding to CoMPP were measured by the oxy–deoxy spectral change, which gave apparent or overall oxygen-binding and -dissociation rate constants (k'_{on} and k'_{off}) according to pseudo-first-order kinetics (Table I). Both k'_{on} and k'_{off} increased with decrease in T_g of the polymer matrix. This result means that physical diffusivity of oxygen in polymer matrices is reflected in the apparent oxygen-binding and -dissociation rate constants to the complex fixed in the polymer membranes. The complex fixed in polymers is an effective probe for estimating the physical properties of polymers.

However, to understand true oxygen-binding kinetic parameters of the complex itself fixed in the membrane, we carried out an in situ flash photolysis study on the bound oxygen with the fixed CoMPP: The recombination reaction of oxygen was completed within 100 μs, to give oxygen-binding and -dissociation rate constants (k_{on} and k_{off}) of the CoMPP complex fixed in the membrane (Table II). In contrast to the apparent or overall oxygen-binding rate constants (k'_{on} and k'_{off}), the true oxygen-binding rate constants, k_{on} and k_{off}, of the complex itself are not influenced by the polymer matrix species. That is, the kinetic parameters estimated by spectroscopy reveal the chemical reactivity of the complex moiety in the membrane as a fixed oxygen carrier.

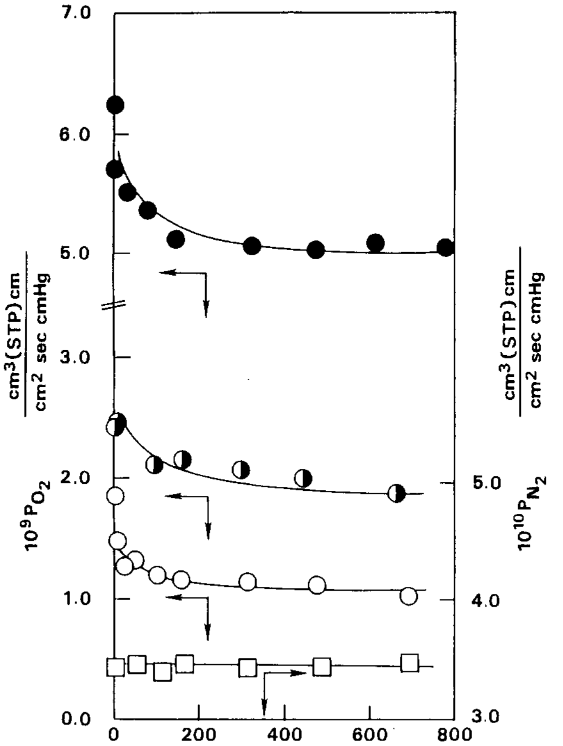

Figure 1. Effect of the upstream oxygen pressure on the oxygen permeability coefficient for the CoMPP membranes at 45 °C. [Co] = 1.3 wt %. (○) BIm; (◑) OIm; (●) LIm. (□) Control plots of the nitrogen permeability coefficient for the CoMPP–BIm membrane.

Analysis of Facilitated Oxygen Transport in the Membranes. Figure 1 shows oxygen and nitrogen permeability coefficients (P_{O_2} and P_{N_2}) in the CoMPP membrane at various upstream oxygen and nitrogen pressures ($p_2(O_2)$, $p_2(N_2)$). While the nitrogen permeability coefficient (P_{N_2}) is small and independent of nitrogen upstream pressure, P_{O_2}'s are large and steeply increase with a decrease in $p_2(O_2)$. This permeation behavior is explained as a carrier-mediated or facilitated transport: The CoMPP complex fixed in the membranes forms an adduct specifically with oxygen, thereby increasing the transport rate of oxygen relative to nitrogen in the upstream. The steep increase in P_{O_2} at low $p_2(O_2)$ derives from the nature of the Langmuir-type oxygen-binding equilibrium (oxygen-sorption isotherm) of this oxygen-carrier system; with decreasing $p_2(O_2)$, more oxygen per pressure unit is sorbed by the membrane than would be predicted by a linear physical sorption isotherm.

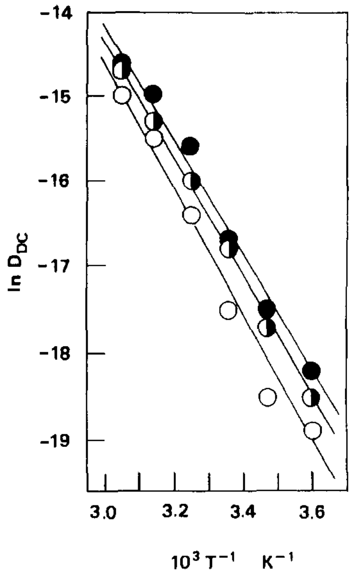

Figure 2. Arrhenius plot of D_{DC} for the CoMPP membranes. (○) BIm; (◑) OIm; (●) LIm.

Paul and Koros[11] and Petropoulos[12] proposed and established a dual-mode transport theory to explain the transport behavior of condensable gases such as carbon dioxide in glassy polymers. In the dual-mode transport model, permeate molecules dissolved and adsorbed in polymer membranes are postulated to diffuse through two distinct pathways—the Henry and Langmuir modes—in parallel and not to execute diffusive movements between the two modes. Recently, a mathematical modification of this dual-mode transport theory was proposed, where new expressions for the permeation and time lag were presented, including the exchanging movements of permeate molecules between dissolved and adsorbed modes.[8,9] On the basis of this modified theory, we analyzed in this paper the facilitated oxygen transport behavior by the following dual-mode transport model.

Diffusive mobility of a permeate molecule in a polymer membrane in this transport model is expressed by four kinds pathways: diffusion for the Henry-type physical permeation (suffix DD), diffusion from the polymer matrix to the CoMPP complex as a fixed carrier (suffix DC), diffusion from the fixed carrier to the polymer matrix (suffix CD), and diffusion for the hopping between the fixed carriers (suffix CC). The total flux can be given by the equation[11]

$$J = J_{DD} + J_{DC} + J_{CD} + J_{CC} \tag{3}$$

The total flux is rewritten as[8]

$$J = -D_{DD}\frac{\partial C_D}{\partial x} - D_{CD}\frac{\partial C_C}{\partial x} - D_{DC}\left[\frac{\partial C_D}{\partial x}\left(1 - \frac{C_C}{C_C'}\right) + \frac{C_D}{C_C'}\frac{\partial C_C}{\partial x}\right] - D_{CC}\frac{\partial C_C}{\partial x} \tag{4}$$

where D is the diffusion coefficient, C_D is the equilibrium concentration of gas dissolved in the polymer, C_C is the equilibrium concentration of gas adsorbed on the carrier moiety, and C_C' is the saturated amount of oxygen reversibly bound to the carrier.

From the relation between C_C and C_D

$$C_C = \frac{RC_D}{1 + \alpha C_D} \tag{5}$$

Here, $R = C_C'K/k_D$ and $\alpha = K/k_D$. Equation 4 becomes

$$J = -\left[D_{DD} + D_{DC}\left(1 - \frac{\alpha C_D}{1 + \alpha C_D}\right) + \left(D_{CC} + D_{CD} + D_{DC}\frac{C_D}{C_C'}\right)\frac{R}{(1 + \alpha C_D)^2}\right]\frac{\partial C_D}{\partial x} \tag{6}$$

After integrating from C_1 ($=k_D p_1$) to C_2 ($=k_D p_2$), one obtains the permeability coefficient as follows:

$$P = k_D D_{DD} + \frac{C_C'KD_{CC}}{(1 + Kp_2)(1 + Kp_1)} + \frac{C_C'KD_{CD} - k_D D_{DC}}{(1 + Kp_2)(1 + Kp_1)} + \frac{2k_D D_{DC}}{K(p_2 - p_1)} \ln \frac{1 + Kp_2}{1 + Kp_1} \tag{7}$$

k_D is solubility coefficient according to Henry's law, K is the oxygen-binding equilibrium constant, p_1 is the downstream gas pressure, and p_2 is the upstream gas pressure. p_1 is approximated to be zero.

$$P = k_D D_{DD} + \frac{C_C'KD_{CC}}{1 + Kp_2} + \frac{C_C'KD_{CD} - k_D D_{DC}}{1 + Kp_2} + \frac{2k_D D_{DC}}{Kp_2} \ln (1 + Kp_2) \tag{8}$$

That is, P is equal to the sum of the first term representing the Henry mode attributed to the physical permeation through the polymer matrix, the second term representing the Langmuir mode attributed to the specific binding and diffusion of oxygen to and from the CoMPP complex as a fixed oxygen carrier, and the third term representing the additive Langmuir mode attributed to the exchanging term between the first and second terms.

$k_D D_{DD}$ in eq 8 was determined by extrapolating a P vs $1/(1 + Kp_2)$ plot to the intercept. D_{DD} and D_{CC} were calculated by using eq 9,[9] in which A represents the exchange term parameter. Introduction of D_{DD} and D_{CC} in eq 8 gave D_{CD} and D_{DC}.

$$P = k_D D_{DD} + \frac{C_C'KD_{CC}}{1 + Kp_2} + \frac{2C_C'KA}{Kp_2} \ln (1 + Kp_2) \tag{9}$$

Effect of the Polymer Matrix on the Oxygen Diffusion. The dual-mode transport parameters were determined by using eq 8 and are listed in Table II. The P_{O_2} vs $p_2(O_2)$ curves are calculated on the basis of the obtained transport parameters and are drawn as the solid line in Figure 1. The experimental plots agree with the solid lines, which supports the modified dual-mode transport of oxygen in the membrane as represented in eq 8 and a pathway of oxygen permeation via the fixed oxygen carrier.

The diffusion coefficients in Table II indicate the following. (i) The four coefficients are in the order $D_{DD} > D_{DC} > D_{CD} > D_{CC}$, which is in accordance with their definition, i.e., the contribution of the oxygen-binding reaction step to and from the fixed carrier: e.g., $k_{on}/k_{off} \sim D_{DC}/D_{CD}$. (ii) Not only D_{DD} but also D_{CD} and D_{DC}, which describe the exchanging mode between the polymer matrix and the fixed carrier, increase with the decrease in T_g or the increase in the free volume of the polymer matrix. (iii) The oxygen diffusion coefficient for the hopping between the fixed carriers, D_{CC}, is independent of the polymer matrix species.

Examples of Arrhenius plots of the diffusion coefficients are shown in Figures 2 and 3, and the activation energies for the diffusion process are given in Table III. The activation energy increases in the order $\Delta E_{CC} > \Delta E_{CD} > \Delta E_{DC} > \Delta E_{DD}$, which agrees with the contribution of the oxygen-binding reaction to each diffusion process. The

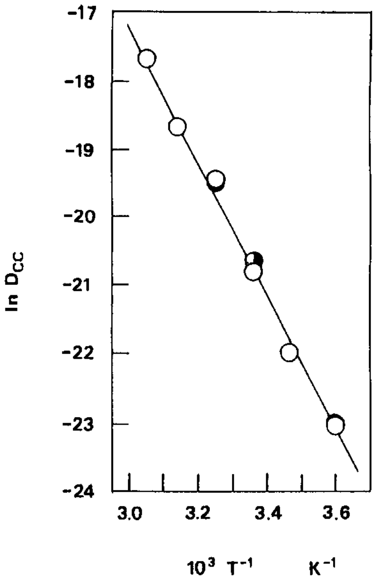

Figure 3. Arrhenius plot of D_{CC} for the CoMPP membranes. (○) BIm; (◑) OIm; (●) LIm.

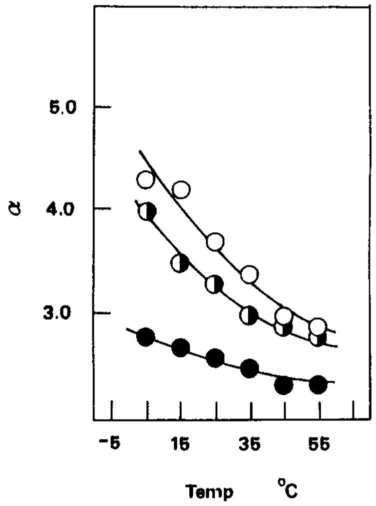

Figure 4. Dependence of the oxygen permselectivity on temperature for the CoMPP membrane at $p_2(O_2)$ = 600 mmHg. (○) BIm; (◑) OIm; (●) LIm.

Table III
Activation Energies[a] for the Oxygen Diffusion Coefficients in the CoMPP Membranes

polymer	ΔE_{DD}	ΔE_{DC}	ΔE_{CD}	ΔE_{CC}
BIm	12	15	17	20
OIm	11	14	16	20
LIm	10	14	16	20

[a] kcal/mol.

ΔE_{CC} values for the postulated diffusion process of hopping of oxygen between the fixed carriers are the largest, which suggests an activation energy barrier for the direct hopping between the fixed carriers or a chemical oxygen-binding reaction via the carrier is a rate-determining step of this facilitated oxygen transport.

Oxygen Permselectivity in the CoMPP Membrane. Figure 4 shows the effect of temperature on the oxygen/nitrogen permselectivity (α) in the CoMPP membrane at $p_2(O_2)$ = 600 mmHg. The α values decrease with temperature, since the oxygen transport is governed by the physical permeation through the polymer matrix at high upstream oxygen pressures. Figure 5 shows the α values at $p_2(O_2)$ = 5 mmHg which correspond to a facilitation efficiency in the oxygen transport. The α-temperature relationships have minima at ca. 30 °C. The values strongly decrease with temperature to ca. 30 °C simply because the physical permeation reduces the permselectivity at higher temperature and because the oxygen-binding equilibrium constant K of the fixed carrier decreases with temperature (see negative ΔH value for the oxygen binding in Table I). However, above the unsuited temperature, the oxygen-binding and -dissociation rate constants increase and the kinetic contribution of the fixed carrier is enhanced with temperature. The permselectivity is related to binding affinity and diffusivity of oxygen to and through the fixed carrier and nitrogen permeability through the polymer matrix pathway.

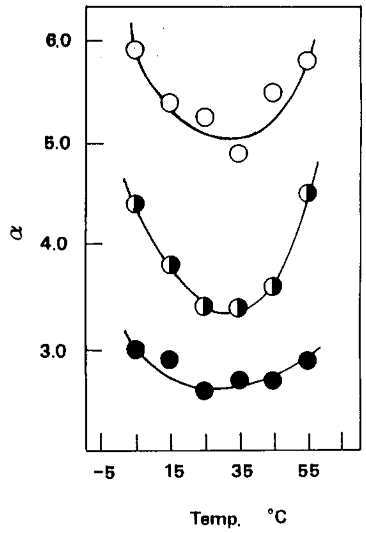

Figure 5. Dependence of the oxygen permselectivity on temperature for the CoMPP membrane at $p_2(O_2)$ = 5 mmHg. (○) BIm; (◑) OIm; (●) LIm.

Acknowledgment. This work was partially supported by a Grant-in-Aid for Scientific Research from the Ministry of Education, Science, and Culture, Japan.

References and Notes

(1) Nishide, H.; Ohyanagi, M.; Okada, O.; Tsuchida, E. *Macromolecules* **1986**, *19*, 444.
(2) Nishide, H.; Ohyanagi, M.; Okada, O.; Tsuchida, E. *Macromolecules* **1987**, *20*, 417.
(3) Tsuchida, E.; Nishide, H.; Ohyanagi, M.; Kawakami, H. *Macromolecules* **1987**, *20*, 1907.
(4) Tsuchida, E.; Nishide, H.; Ohyanagi, M.; Okada, O. *J. Phys. Chem.* **1988**, *92*, 6461.
(5) Ohyanagi, M.; Nishide, H.; Okada, O.; Tsuchida, E. *Macromolecules* **1988**, *21*, 1590.
(6) Nishide, H.; Ohyanagi, M.; Okada, O.; Tsuchida, E. *Macromolecules* **1988**, *21*, 2910.
(7) Nishide, H.; Kawakami, H.; Suzuki, T.; Azechi, Y.; Tsuchida, E. *Macromolecules* **1990**, *23*, 3714.
(8) Barrer, R. M. *J. Membr. Sci.* **1984**, *18*, 25.
(9) Fredrickson, G. H.; Helfand, E. *Macromolecules* **1985**, *18*, 2201.
(10) Cussler, E. L.; Aris, R.; Bhown, A. *J. Membr. Sci.* **1989**, *43*, 149.
(11) Paul, D. R.; Koros, W. J. *J. Polym. Sci., Polym. Phys. Ed.* **1976**, *27*, 177.
(12) Petropoulos, J. H. *J. Polym. Sci., Part A-2* **1970**, *8*, 1797.

Registry No. O_2, 7782-44-7.